Effect of window reflection on gyrotron operation

T. M. Antonsen Jr., S. Y. Cai, and G. S. Nusinovich

Citation: Physics of Fluids B **4**, 4131 (1992); doi: 10.1063/1.860320
View online: http://dx.doi.org/10.1063/1.860320
View Table of Contents: http://scitation.aip.org/content/aip/journal/pofb/4/12?ver=pdfcov
Published by the AIP Publishing

Effect of window reflection on gyrotron operation

T. M. Antonsen, Jr.,[a] S. Y. Cai,[b] and G. S. Nusinovich
Laboratory for Plasma Research, University of Maryland, College Park, Maryland 20742

(Received 6 March 1992; accepted 13 August 1992)

A simple nonlinear theoretical model is developed to study the effects of small reflections from gyrotron output windows on gyrotron operation. The results obtained from this model show that when the product of the reflection coefficient and the delay time is small enough the gyrotron oscillates stably, and the output frequency will vary smoothly with changes in the cold cavity frequency. When the product is large, however, the output frequency jumps when the cold cavity frequency changes. Further, the reflection can, under certain conditions, cause the gyrotron to become unstable and the output frequency will have a spectrum that either consists of periodically spaced discrete lines, a dense set of narrow lines, or even a broadband spectrum. The width of this spectrum is inversely proportional to the delay time.

I. INTRODUCTION

In a number of experiments[1,2] with long-pulsed gyrotrons there have been observations of slow time variations in the operating frequency that could be associated with gradual heating of the gyrotron cavity, collector, and output window. The time variation of the frequency is characterized by a sequence of discrete jumps, indicating that reflections from the output window are influencing the operation. The reflection of microwaves from the output window can also affect the starting and optimal currents of the operating mode and mode competition. These issues were first discussed in the context of gyrotrons by Jödicke.[3] It seems quite obvious that similar effects may be caused by reflection of microwaves from any part of the microwave transmission lines, which include, usually, mode converters, elbows, and miter bends, as well as the input windows to the plasma vessel (see, for example, Refs. 4 and 5 and the cited literature). For long-pulsed gyrotrons, where built-in quasioptical converters are usually used,[6] such long-line effects are generally not as important as for gyrotrons, in which a microwave power radiated from the cavity is directed via a tapered waveguide to the output window and, then, also via the set of waveguides to the plasma installation.[5]

At present, an intensive study of ceramic output windows for powerful long-pulsed or continuous wave (cw) gyrotrons have been carried out.[7,8] However, these studies mainly concentrated on mechanical properties of ceramic windows, which absorb part of the transmitted microwave power. A general analysis of the temperature and stress distributions in the gyrotron output window is given in Ref. 9, and a quite general approach to the analysis of window reflections was carried out by Nickel *et al.*[10] However, the nonstationary effects of window reflections on gyrotron operation were not studied.

In most gyrotrons the thickness of the output window is matched to the operating wavelength, in order to make the reflection coefficient as small as possible. In such cases two kinds of rf power reflection may be important. The first one is a nonzero reflection of parasitic modes, whose eigenfrequencies differ slightly from that of the operating mode but can still be at resonance with the electron cyclotron frequency or its harmonics. The second one is the nonzero reflection of waves that appear due to transformation of the operating mode in the irregular output waveguide, such that the signal arriving at the window consists of a mixture of different transverse modes. Such waves, of course, have the same frequency as the operating mode but different axial wave numbers that cause a finite reflection of their power.

The first effect can diminish the starting current of parasitic modes and, therefore, in order to suppress these modes one must increase the stability reserve of the operating mode in mode competition.[11,12] So, we can assume that the appropriate choice of gyrotron parameters and the start-up scenario enables us to suppress excitation of parasitic modes.

The second effect is inherent in all conventional gyrotrons, where in a tapered output waveguide the conversion of the operating mode into waves with different radial indices takes place. This problem can only be mitigated by optimization of such tapering.[13]

II. EFFECTS OF WINDOW REFLECTION ON SINGLE-MODE OPERATION

As we discussed in the previous section, there are a number of possible causes of microwave reflection from the output section back to the interaction region of a gyrotron. In this section we present a simple nonlinear model, which allows one to study the effects of output reflection on the evolution of a single mode of the interaction region. This model complements the method used in the past to treat reflections based on Reike diagrams.[1] This previous method determines by a combination of numerical and graphical techniques the output power and frequency of the gyrotron for a given complex reflection coefficient. While the method treats certain aspects of the problem with great precision, it is computationally intensive, and it

[a] Also at the Departments of Electrical Engineering and Physics.
[b] Permanent address: Science Application International Corporation, Applied Physics Division, 1710 Goodridge Dr., McLean, Virginia 22102.

 0899-8213/92/124131-09$04.00

requires the assumption that the radiation is monochromatic. We shall see from our simple model that this last assumption is not always satisfied, and indeed, reflections can cause an otherwise stable free running oscillator to become unstable and chaotic.

We start the analysis by expressing the electric field in the cavity as

$$\mathbf{E}(\mathbf{r})=\hat{\mathbf{E}}(\mathbf{r})A(t)\exp\left(-i\int^{t}\omega_0(t')dt'\right)+\text{c.c.}, \tag{1}$$

where $\hat{\mathbf{E}}(\mathbf{r})$ is the empty cavity field profile, $A(t)$ is its complex time-dependent amplitude, and $\omega_0(t)$ is the cold cavity resonant frequency, assuming no spurious reflections. Here we have allowed the cold cavity frequency to depend on time, reflecting possible changes in size or shape of the cavity during a long pulse. These changes will be presumed to be small, so that only the cavity frequency is changed and not the field structure.

In the case of a high-Q cavity, where Q is the usual quality factor, the field amplitude A changes on a much longer time scale than the electron transit time through the cavity. The evolution of the amplitude $A(t)$ is then governed by a simple nonlinear equation,

$$\frac{dA(t)}{dt}=\Gamma(|A|)A(t)-\frac{\omega_0}{Q}A(t), \tag{2}$$

where $\Gamma(|A|)$ is the complex nonlinear growth rate due to the interaction of the radiation and the electron beam. The functional form of Γ is determined by solving for trajectories of the electrons in the prescribed axial field profile of the cavity mode, for example, one could adopt the standard Gaussian profile ansatz. The real part of Γ is the gain and the imaginary part of Γ is the frequency shift. That the nonlinear gain depends only on the amplitude of the radiation follows from the fact that electrons are homogeneously distributed in initial gyrophases on injection into the interaction region, and, thus, the phase of the radiation amplitude does not affect, for example, the rate at which power is extracted from the beam. The second term on the right-hand side of Eq. (2) describes the cavity losses that we will assume are dominated by diffraction out of the interaction region. Here ω_0 is the cold cavity frequency of oscillation whose time dependence can be ignored in Eq. (2) [but not in Eq. (1)].

The presence of spurious reflection from the output region will modify the loss term in Eq. (2). If the time for the signal to travel from the cavity to the point of reflection and back is T_d, the reflected wave in the cavity at the time t will have an amplitude given by $\rho\exp(i\theta)A(t-T_d)$, where ρ and θ_r are the magnitude and phase of the reflection coefficient at the point of reflection, and

$$\theta=\theta_r+2\int_{\text{cavity}}^{\text{reflector}}dz\,k_z[\omega_0(t),z] \tag{3}$$

is the total phase shift for the complete round trip of the wave. In terms of this phase shift, the delay time is

$$T_d=\left(\frac{\partial\theta}{\partial\omega_0}\right). \tag{4}$$

Since the second term in Eq. (3) for the round trip phase will be large if the cavity and reflector are separated by a large distance, it is important to retain the time dependence of the various parameters that affect this phase. In particular, changes in the frequency of the radiation will be important. The resulting time variation of this phase will influence the evolution of the complex amplitude in a way that will be discussed subsequently.

The addition of reflection modifies Eq. (2) in the following way:

$$\frac{dA(t)}{dt}=\Gamma(|A|)A(t)-\frac{\omega_0}{Q}[A(t)+\rho\exp(i\theta)A(t-T_d)]. \tag{5}$$

Thus, the amplitude of the radiation in the cavity is described by a nonlinear differential delay equation.

As we have discussed in the previous section, the reflection coefficient ρ for a well-matched output is expected to be small. Therefore, the reflection term in Eq. (5) will be treated as a small perturbation to the zero reflection solution of Eq. (2). Correspondingly, we can express the complex amplitude of the rf field $A(t)$ as

$$A(t)=(a_0+\delta a)\exp(i\{\Phi+\text{Im}[\Gamma(a_0)]t\}), \tag{6}$$

where $A_0(t)=a_0\exp\{i\,\text{Im}[\Gamma(a_0)]t\}$ is the unperturbed free running solution of Eq. (2) with constant amplitude a_0, and the quantity $-\text{Im}[\Gamma(a_0)]$ is the beam-induced frequency shift. (This quantity is plotted, for example, in Ref. 14.) The condition for such a free running solution is determined by power balance, and follows from Eq. (2),

$$\text{Re}[\Gamma(a_0)]=\frac{\omega_0}{Q}. \tag{7}$$

The quantities δa and Φ are perturbations of the amplitude and phase, respectively. For a small reflection coefficient the perturbation of the amplitude will be small, but the perturbation to the phase can become large after a sufficiently long time.

We then substitute Eq. (6) into Eq. (5), expand all quantities to the first order in δa, $d\Phi/dt$ and ρ, and use condition (7) to obtain equations for δa and Φ,

$$\frac{d\delta a(t)}{dt}=-\gamma_s\delta a(t)-a_0\frac{\omega_0}{Q}\rho\cos[\theta'+\Phi(t-T_d)-\Phi(t)], \tag{8a}$$

$$\frac{d\Phi(t)}{dt}=\gamma_1\frac{\delta a(t)}{a_0}-\frac{\omega_0}{Q}\rho\sin[\theta'+\Phi(t-T_d)-\Phi(t)], \tag{8b}$$

where $\theta'=\theta-\text{Im}[\Gamma(a_0)]T_d$, and the coefficients γ_s and γ_1 are defined by the relations

$$\gamma_s = -\mathrm{Re}\left(a_0 \frac{\partial \Gamma}{\partial a_0}\right) = -\frac{\omega_0}{Q} \frac{d \ln \mathrm{Re}[\Gamma(a_0)]}{d \ln a_0},$$

$$\gamma_1 = \mathrm{Im}\left(a_0 \frac{\partial \Gamma}{\partial a_0}\right) = \frac{\omega_0}{Q} \frac{1}{\mathrm{Re}[\Gamma(a_0)]} \frac{d \,\mathrm{Im}[\Gamma(a_0)]}{d \ln a_0}.$$

Here γ_s is the decay rate for the amplitude of the radiation in the free running oscillator ($\gamma_s > 0$ for a stable equilibrium), and γ_1 is the coefficient giving the change in beam-induced frequency shift for a given change in radiation amplitude.

Equations (8a) and (8b) describe processes occurring on two different time scales: the time scale for decay of the amplitude of the radiation in the free running oscillator and the time scale for the return of the radiation from the point of reflection. As an order of magnitude estimate, the preceding definitions indicate that the rates γ_s and γ_1 (describing the relaxation to equilibrium in the absence of reflections) scale as the empty cavity decay rate,

$$\gamma_s \sim \gamma_1 \sim \omega_0/Q.$$

This follows from the fact that these rates are defined in terms of derivatives of the nonlinear gain with respect to the logarithm of the radiation amplitude, and by the equilibrium relation (7) the nonlinear gain scales as the empty cavity decay rate. Figures 1(a) and 1(b) show level curves of the dimensionless coefficients $G_s = Q\gamma_s/\omega_0$ and $G_1 = Q\gamma_1/\omega_0$, in the detuning versus field amplitude plane for the case of a Gaussian field profile. Here detuning is defined as $\delta = (\omega_0 - \Omega_0/\gamma_0) r_0/v_{z0}$, and the dimensionless field amplitude is defined by $a_0 = qr_0E/m\gamma_0 v_{\perp 0} v_{z0}$, where Ω_0 is the nonrelativistic cyclotron frequency, γ_0 is the relativistic factor, r_0 is the half-width of the Gaussian, v_{z0} and $v_{\perp 0}$ are the injected axial and transverse velocities, E is the peak electric field, and q and m are the electron charge and mass. The plot corresponds to a value of the dimensionless interaction length $\mu_L = \Omega_0 r_0 v_0^2/(\gamma_0 v_{z0} c^2) = 10$. Also shown in Fig. 1(c) are level curves of the perpendicular efficiency for the same parameters.

We now assume that the delay time T_d is much longer than the cavity decay time, such that

$$\omega_0 T_d/Q \gg 1.$$

In this case, Eq. (8a) indicates that the effect of the reflection is to induce relatively small fluctuations in the amplitude of the radiation (recall that we have already assumed that the reflection coefficient, ρ, is small) with a characteristic time scale of the delay time. Since the time scale of the fluctuations is the delay time, the amplitude can be calculated by dropping the left-hand side of Eq. (8a), which is small in comparison to the first term on the right-hand side of Eq. (8a),

$$\delta a(t) = -a_0 \frac{\omega_0}{Q\gamma_s} \rho \cos[\theta' + \Phi(t - T_d) - \Phi(t)]. \qquad (9)$$

This equation can then be inserted in Eq. (8b) to obtain a first-order differential delay equation for the radiation phase,

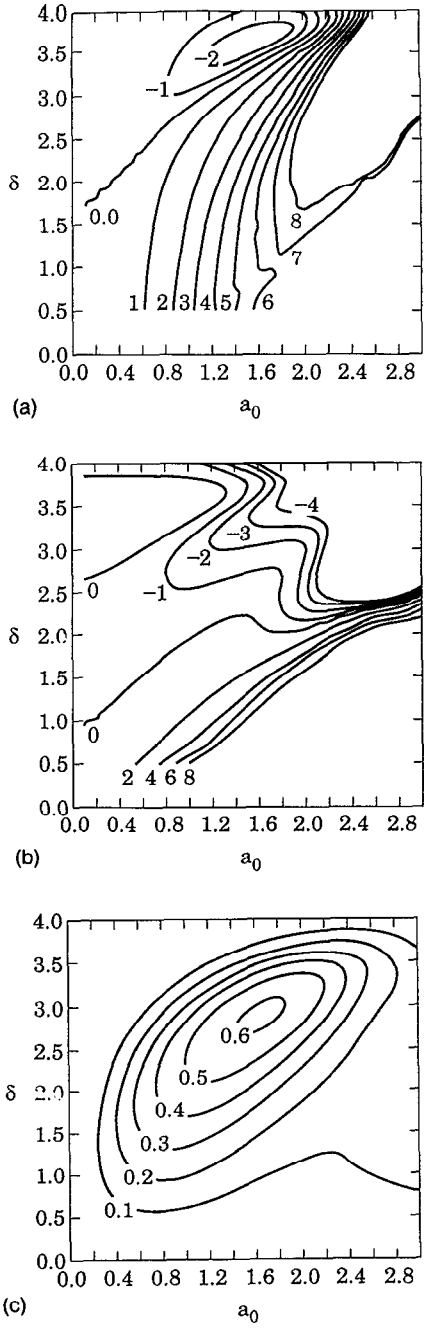

FIG. 1. Level curves of (a) G_s, (b) G_1, and (c) perpendicular efficiency in the detuning versus field amplitude plan for the case of a Gaussian field profile.

$$\frac{d\Phi(t)}{dt} = -\frac{\omega_0 \bar{\gamma}}{Q\gamma_s} \rho \cos[\theta'' + \Phi(t - T_d) - \Phi(t)]. \qquad (10)$$

Here $\bar{\gamma} = \sqrt{\gamma_1^2 + \gamma_s^2}$ and $\theta'' = \theta' - \tan^{-1}(\gamma_s/\gamma_1)$.

As stated, the preceding derivation assumes that the rates γ_s and γ_1 scale as the empty cavity decay rate. While this is, in general, true, the numerical coefficient of this scaling can become quite small for equilibria in the hard excitation region. It can be seen from Figs. 1(a) and 1(c) that the coefficient γ_s vanishes along a line that cuts through the high efficiency region of the detuning-field amplitude plane. This situation is further illustrated in Fig. 2,

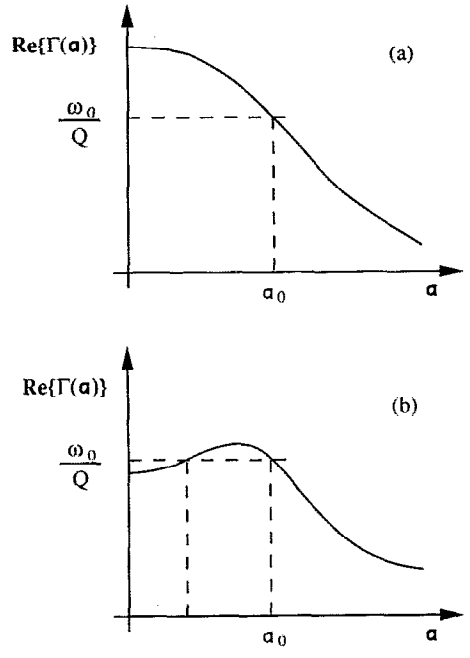

FIG. 2. Graphical determination of the free-running equilibrium in (a) the soft excitation case and (b) the hard excitation case.

where schematic plots of the nonlinear gain versus radiation amplitude for parameters of detuning and normalized interaction length giving soft [Fig. 2(a)] and hard excitation [Fig. 2(b)] are shown. The amplitude of free running oscillations in these cases is determined by the intersection of the gain and loss curves [cf. Eq. (7)]. In the case of Fig. 2(a) (soft excitation) for the given parameters, there is a single equilibrium solution. The slope of the gain curve at this equilibrium is nonzero, and hence, the amplitude decay rate will be of the same order as the empty cavity decay rate. For the case of Fig. 2(b) (hard excitation) there are two equilibrium solutions for the given parameters. The solution with the smaller value of amplitude is unstable, $\gamma_s<0$, while the solution with the larger value is stable, $\gamma_s>0$. Thus, a free running oscillator in the hard excitation regime will choose the larger value of amplitude. The amplitude decay rate is again determined by the slope of the gain curve for this equilibrium. As the parameters of the oscillator, such as detuning are varied, the gain curve's shape changes and the equilibrium amplitude varies. For example, increasing the detuning lowers the gain curve and eventually the oscillator finds itself in an equilibrium at the peak of the gain curve. In this case the amplitude decay rate goes to zero, while γ_1 is nonzero.

To treat the case of small γ_s we compare the terms on the right-hand side of Eqs. (8a) and (8b). We note that the two right-hand sides are similar, except that γ_s (which is now assumed to be small) appears in Eq. (8a) and γ_1 (which is still large) appears in Eq. (8b). Thus, as one considers the effects of progressively larger reflection coefficients, the first interesting case is one in which the second term on the right-hand side of Eq. (8b) is smaller than the first. We, thus, drop the second term from Eq. (8b), solve for $\delta a(t)$ as in terms of $d\Phi/dt$ and substitute in Eq. (8a). This gives

$$\left(\frac{d}{dt}+\gamma_s\right)\frac{d\Phi}{dt}+\frac{\omega\gamma_1}{Q}\rho\cos[\theta'+\Phi(t-T_d)-\Phi(t)]=0. \tag{11}$$

A single equation, which encompasses both Eqs. (10) and (11), can be obtained by replacing γ_1 by $\bar{\gamma}$ and θ' by θ'' in Eq. (11).

Finally, we caution that one must always check to see that the basic assumption of small-amplitude fluctuations, $\delta a/a_0\ll 1$, remains valid. If the amplitude fluctuations become too large, then the linearizations in Eqs. (8) break down. One could improve the present model by including the next term (quadratic in δa) in the Taylor expansion of the nonlinear gain in Eq. (8a). This will introduce another parameter, and perhaps different and interesting behavior. For the time being, however, we will investigate the solutions of Eq. (11).

We now simplify Eq. (11) by introducing the normalizations

$$\tau=t/T_d, \tag{12a}$$

$$\mu=\gamma_s T_d, \tag{12b}$$

and

$$R=\omega_0\bar{\gamma}\rho T_d^2/Q, \tag{12c}$$

which yields

$$\left(\frac{d}{d\tau}+\mu\right)\frac{d\Phi}{d\tau}+R\cos[\theta''+\Phi(\tau-1)-\Phi(\tau)]=0. \tag{13}$$

Note that this is the equation for a damped nonlinear pendulum under the influence of a gravitational field, which changes its direction based on past angular locations of the pendulum. The equation contains three dimensionless parameters: the dimensionless amplitude decay rate μ, the normalized reflection amplitude R, and the reflection phase,

$$\theta''=\theta_r+2\int_{\text{cavity}}^{\text{reflector}} dz\, k_z[\omega(t),z]-\text{Im}[\Gamma(a_0)]T_d$$
$$-\tan^{-1}(\gamma_s/\gamma_1). \tag{14}$$

The solutions of Eq. (13) determine the instantaneous output frequency of the oscillator. In particular, the frequency is found from Eqs. (1) and (6) to be the sum of the cold cavity frequency, the beam-induced frequency shift for a free running oscillator, and the reflection induced shift governed by Eq. (13),

$$\omega=\omega_0(t)-\text{Im}[\Gamma(a_0)]-T_d^{-1}\frac{d\Phi}{d\tau}. \tag{15}$$

Thus, solutions of Eq. (13) will produce frequency fluctuations or broadening on the scale of the inverse of the delay time.

In general, Eq. (13) requires a numerical solution. However, some progress can be made by looking for steady

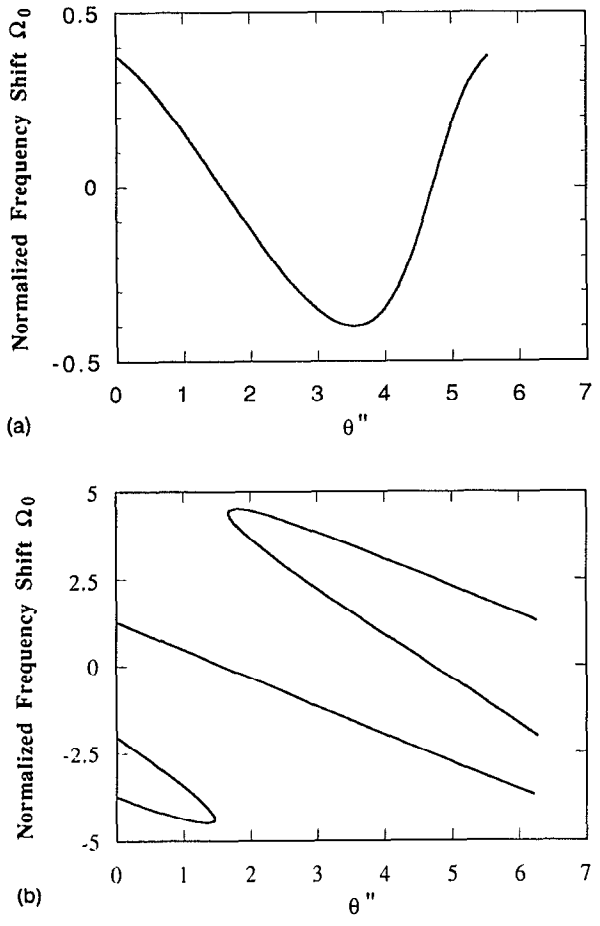

FIG. 3. Dependence of the equilibrium frequency shift, Ω_0, induced by the window reflection on the phase θ''. (a) $R/\mu=0.4$, showing that the frequency shift is a single function of θ''. (b) $R/\mu=4.5$, showing that Ω_0 is a multiple value function of θ''.

equilibria and examining their stability. The frequency shift of an equilibrium state of Eq. (13) satisfies the relation

$$\Omega_0 \equiv -\frac{d\Phi(\tau)}{d\tau} = \frac{R}{\mu}\cos(\theta''+\Omega_0). \tag{16}$$

With R/μ and θ'' specified, Eq. (16) possesses an odd number of solutions for Ω_0. Such multiple solutions can also be obtained by using the Reike diagram technique.[1] If $|R/\mu|<1$ (weak reflections) there is a single solution. For larger values of $|R/\mu|$, there will be more solutions corresponding to standing waves with different numbers of modulations between the reflector and the cavity. This is illustrated in Figs. 3, where the normalized equilibrium frequency shift Ω_0 is plotted versus θ'' for two different values of R/μ. Note that to be in the weak reflection regime, $|R/\mu|<1$, it is required that the product of the reflection coefficient and the delay time be small, not simply that the reflection coefficient be small.

The dependence of Ω_0 on θ'' is important since it determines the evolution of the output frequency of the gyrotron as the phase θ'' is adiabatically varied. By adiabatically, we mean on a time scale much slower than the reflection delay time T_d. For example, if the cavity wall heats up and changes shape, the phase θ defined in Eq. (3), and hence θ'', will change due to the changing cold cavity frequency. Alternatively, changes of voltage or magnetic field that change the beam-induced frequency shift that appears in Eq. (14) will change the phase θ''. In the case of weak reflection [Fig. 3(a)], the normalized frequency varies smoothly with θ'', being essentially a constant (zero) with periodic modulations of order R/μ. The resulting output frequency, given by Eq. (15) with $d\Phi/dt$ replaced by $-\Omega_0$, will then smoothly track the changing cold cavity frequency. In the case of strong reflection ($|R/\mu|>1$) as θ'' is varied, the normalized frequency cannot change continuously, but must suffer jumps, as illustrated in Fig. 3(b). As a result, the output frequency will track the changing cold cavity frequency by making a combination of continuous changes punctuated by steps, which scale roughly as $2\pi/T_d$. For extremely large $|R/\mu|$ values, Eq. (16) requires that the quantity $\Omega_0+\theta''$ is nearly constant between steps. This implies from Eqs. (15) and (4) that the output frequency is nearly constant between the steps.

So far we have considered the properties of equilibrium states of gyrotron operation in the presence of a small output window reflection. These equilibrium states can be stable or unstable when the states are subject to a small perturbation. To study the stability properties of the equilibrium states, we let

$$\Phi(\tau) = -\Omega_0\tau+\delta\Phi(\tau)$$
$$= -\Omega_0\tau+\mathrm{Re}[\delta\Phi_0\exp(-i\nu\tau)], \tag{17}$$

where Ω_0 is the equilibrium frequency shift given by Eq. (16), $\delta\Phi_0$ is a small constant, ν is the complex frequency of the perturbed phase, and the instantaneous frequency shift due to the reflection is given by

$$\Omega \equiv \frac{d\Phi(\tau)}{d\tau}. \tag{18}$$

The dispersion function determining ν can be obtained by substitution of Eq. (17) in Eq. (13) and linearization of the equation to the first order of $\delta\Phi(\tau)$,

$$D(\nu) = \nu^2+i\mu\nu+C[\exp(i\nu)-1]=0, \tag{19}$$

where $C=R\sin(\theta''+\Omega_0)$. Note that the dispersion function $D(\nu)$ depends only on two parameters, μ and C, and thus the stability of an equilibrium depends only on these two parameters. A straightforward Nyquist stability analysis is then employed to obtain the stable and unstable domains in the μ-C plane. The result is plotted in Fig. 4, where the lower boundary of the stable region is given by $C=-\mu$ and the upper boundary is given by the lowest solution of Eq. (19) for real ν. We see that when $|R/\mu|\leqslant 1$, the equilibrium is always stable. When $|R/\mu|>1$, due to the dependence of C on θ'', the equilibrium can be either stable or unstable, depending on θ''. An example is given in Fig. 5, where the stable equilibrium is depicted by solid lines and the unstable equilibrium by dashed lines.

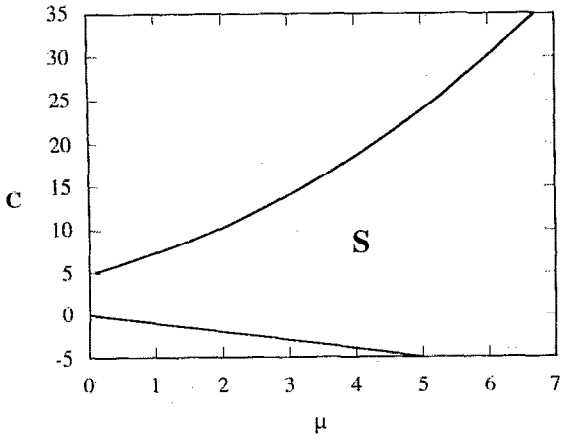

FIG. 4. Stability boundary on the (C-μ) plane. The stable region is indicated by the letter **S**.

To illustrate the behavior of the frequency shift Ω when equilibria are not stable, we picked three sets of parameters with three different reflection coefficients: $\mu=1$, $\theta''=1.6$, and (a) $R=15.0$, (b) $R=21.98$, and (c) $R=23.0$, and solved Eq. (13) numerically for the frequency shift Ω as a function of τ. The corresponding solutions are plotted in Figs. 6(a)–6(c), where the transition from periodic behavior (a) to rather chaotic behavior (c) is illustrated. In none of these cases did the frequency tend to a constant, even though all parameters are fixed. In the first case [Fig. 6(a)] the normalized frequency shift, Ω, became a periodic function of time with a period T_d/α with $\alpha\simeq 0.6$ for the case shown. The resulting output spectrum of the gyrotron, shown in Fig. 7(a), consists of a set of narrow lines with frequencies corresponding to the free running oscillator, plus all harmonics of $2\pi\alpha/T_d$,

$$\omega_m=\omega_0-\mathrm{Im}(\Gamma)+\frac{2\pi m\alpha}{T_d},$$

with $m=0, \pm 1, \pm 2$, etc.

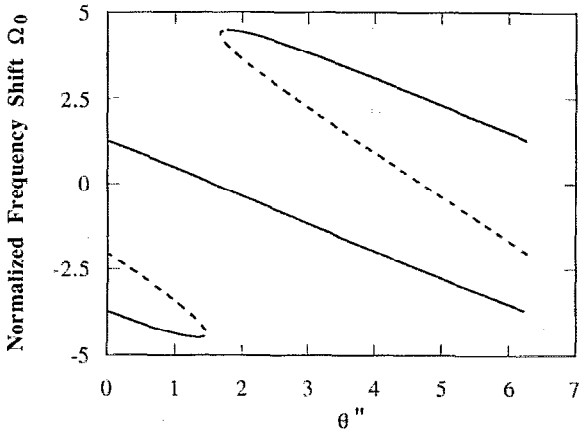

FIG. 5. A special case of Fig. 3(b) with $\mu=1.0$ and $R=4.5$. Here the stable equilibrium is indicated by the solid lines and the unstable equilibrium by the dashed lines.

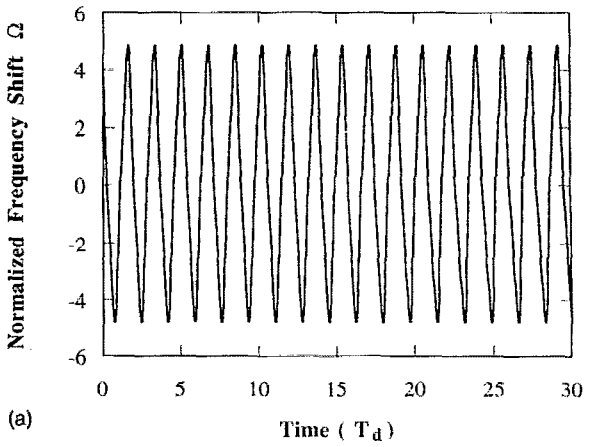

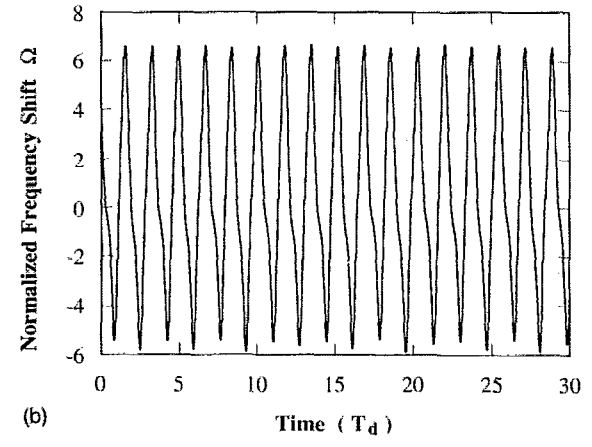

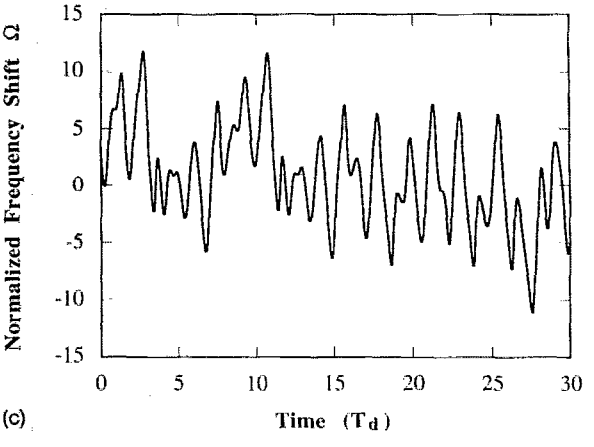

FIG. 6. Time dependence of the frequency shift Ω for (a) $\theta''=1.6$, $\mu=1.0$, and $R=15.0$. The frequency shift Ω is a periodic function of time; (b) $\theta''=1.6$, $\mu=1.0$, and $R=21.98$. The frequency shift Ω is a quasiperiodic function of time; (c) $\theta''=1.6$, $\mu=1.0$, and $R=23.0$. The frequency shift Ω becomes chaotic.

In the second case, with a higher reflection coefficient, the normalized frequency shift, Ω, is a two-frequency quasiperiodic function with normalized frequencies $2\pi\alpha_1/T_d$ and $2\pi\alpha_2/T_d$. In this case the output frequency of the gyrotron consists of a dense set of narrow lines with frequencies

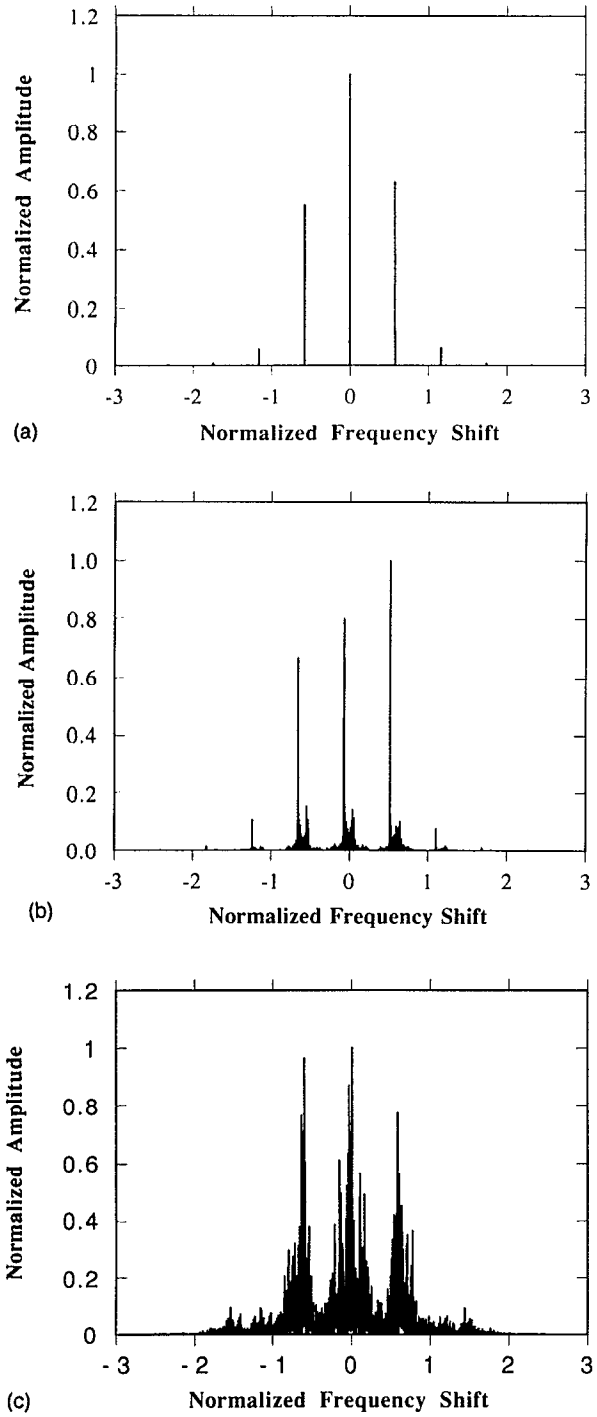

FIG. 7. The corresponding frequency spectra for the three cases shown in Fig. 6.

$$\omega_{m,n}=\omega_0-\mathrm{Im}(\Gamma)+\frac{2\pi(m\alpha_1+n\alpha_2)}{T_d},$$

with m, $n=0, \pm 1, \pm 2$, etc., as is shown in Fig. 7(b). Finally, in the third case with a still higher reflection coefficient the normalized frequency shift appears to be a chaotic function, and the resulting output of the gyrotron will be a broadband spectrum with a width of the order of $2\pi/T_d$ [Fig. 7(c)].

III. DISCUSSION

One of the basic predictions of our model (and other's) is that under certain circumstances the output frequency will suffer jumps, as opposed to changing continuously, as a parameter is changed slowly with time. By slowly we mean on a time scale longer than the reflection delay time. A necessary condition for these jumps is that the parameter $R/\mu > 1$, where R and μ are defined in Eqs. (12b) and (12c). This condition can be satisfied even if the reflection coefficient, itself, is small, provided the other parameters have the requisite size. Another condition for frequency jumping to be observed in an experiment is that the phase delay θ'' is varied over a range of the order of π. The variation of θ'' in an experiment can be a result of the slight variation in the frequency of the free-running gyrotron due to a change in operating parameters, such as voltage, current, or magnetic field (e.g., Ref. 14), and/or gradual heat-up of the gyrotron cavity and the output section between the cavity and output window (e.g., Ref. 2).

In the experiment described in Ref. 14, frequency jumping was observed for the $TE_{4,2,1}$ mode at central frequencies around 127.3 GHz. In this case, since the output window was designed for the $TE_{0,3,1}$ mode at 140 GHz, the window reflection coefficient for the $TE_{4,2,1}$ mode is expected to be large. The experiment observed two jumps in output frequency when the main cavity magnetic field was varied over a range, such that the free-running gyrotron frequency would have varied about 0.2 GHz. To roughly estimate the corresponding change in the delay phase θ'' caused by this 0.2 GHz change in the main frequency, we suppose that the distance between the cavity and the window is about 1 m and the group velocity of the wave in this section is close to the speed of light in vacuum ($T_d \simeq 3.3$ sec). Then the change in phase delay is approximately

$$\Delta\theta'' \sim 4\pi L\, \Delta f/c \sim 2.7\pi,$$

which is about that is needed for the frequency to jump twice.

In the Varian experiment,[15] the gyrotron was designed to operate at 140 GHz in the $TE_{15,2}$ mode. In this experiment, the magnetic field was tuned to achieve optimal efficiency, and thus its μ should be small. Since the experiment was operated in a quasicontinuous wave mode (pulse length of 0.1 sec), the change in the delay phase was mainly caused by the gradual heating of the cavity and the output section. Again, if we assume that the distance between the cavity and the window is 1 m and the wave's group velocity is close to c, then similar to the Massachusetts Institute of Technology (MIT) experiment discussed above, the change in the free-running frequency should be on the order of 0.1 GHz in order for the frequency jumping to be observed. Therefore, the heating of the cavity wall during one pulse duration must cause the wall radius to change 0.07%. This change in the wall radius can usually occur for 140 GHz, 0.5 MW gyrotron if the pulse duration is longer than 50 msec. The gradual heating of the collector can also cause changes in the delay phase. To absorb a 1 MW electron beam, the length of the collector of 4 in. in

diameter can expand during a 100 msec pulse over a quarter-wavelength, causing the phase delay to have a change of about π.

We should point out that the estimations given above are very crude ones. The actual change in the delay phase will depend sensitively on the shape and length of the output section and the method used to cool the cavity and the beam collector. Nevertheless, these estimations shows that our model is qualitatively in agreement with experiments.

IV. CONCLUSION

In this paper, we have studied the effects of one aspect of reflection of microwaves from the output window on gyrotron operations. A simple theoretical model is developed to account for the effect of reflection on a gyrotron, which, in the absence of reflection, operates stably. Our analysis shows that when the product of the reflection coefficient and the delay time is large enough ($|R/\mu|>1$), frequency of the output radiation can jump as the delay phase varies. When gyrotron operation is optimized for highest efficiency, the operation is usually in the hard-excitation regime and is near the boundary of stable gyrotron operation. In this case, the amplitude decay coefficient γ_s (and μ) may be very small. Under these circumstances operation will be very sensitive to window reflection. The frequency jumping phenomenon has been observed in some experiments, where the delay phase was changed due to a gradual heating of the gyrotron output waveguide.

We have also shown that the reflection can cause radiation frequency to be unstable and thereby produce a finite bandwidth in the output spectrum. The bandwidth is inversely proportional to the delay time T_d. We should also point out that although we have considered gyrotron operation specifically in this study, the theoretical model is expected to be rather universal for any low gain oscillators with small output reflection.

ACKNOWLEDGMENT

This work is supported by the U.S. Department of Energy.

APPENDIX: REFLECTION COEFFICIENT OF AN OUTPUT WINDOW

In this appendix, we consider the propagation of a TE wave through a ceramic disk using the boundary conditions that tangential components of electric and magnetic fields of the wave are continuous at the disk boundaries. Using a procedure described elsewhere (e.g., J. Jackson,[16] Chap. 7), one can easily get the following expression for the reflection coefficient:

$$|\rho|=\left|\frac{1-x}{1+x}\right|\frac{2|\sin k_z' d|}{\{1+[(1-x)/(1+x)]^4-2[(1-x)/(1+x)]^2\cos 2k_z' d\}^{1/2}}, \tag{A1}$$

where k_z' is the axial wave number in the ceramic [$k_z'^2=n^2(\omega^2/c^2)-k_\perp^2$, n and $n^2=\epsilon$ are the refractive index and dielectric constant, respectively, $k_\perp$ is the transverse wave number], $x=k_z'/k_z$, where $k_z=(\omega^2/c^2-k_\perp^2)^{1/2}$ is the axial wave number in the empty waveguide, and d is the thickness of the disk.

In a similar manner, one can also consider the double-disk configuration, which is preferable for long-pulsed/cw operation due to the possibility of providing an intensive window surface cooling. The corresponding expression for the total reflection coefficient of a double disk window is

$$|\rho|=2\left|\sin\alpha\,\frac{(x^2-1)[(1+x)^2\cos(\alpha+\beta)-(1-x)^2\cos(\alpha-\beta)]}{[(1+x)^2-(1-x)^2e^{i2\alpha}]^2-[(1-x^2)(1-e^{i2\alpha})]^2\exp(i2\beta)}\right|, \tag{A2}$$

where $\alpha\equiv k_z' d$, $\beta\equiv k_z L$, and L is the separation between disks.

According to Eq. (A1) the single-disk window is matched ($|\rho|=0$) when its thickness satisfies the condition

$$\alpha=\alpha_0=m\pi, \tag{A3}$$

where m is an integer. In a double-disk configuration, besides this obvious condition, another possibility to discriminate window reflections exists. As it follows from expression (A2), the total reflection coefficient can be also set to zero when the distance between the disks satisfies the condition

$$\frac{\cos(\alpha_0+\beta_0)}{\cos(\alpha_0-\beta_0)}=\left(\frac{1-x}{1+x}\right)^2. \tag{A4}$$

Let us estimate the sensitivity of the reflection coefficient of the matched output window with respect to perturbations in k_z', d, and L in all cases discussed above. In a single-disk window the perturbation in α [$\alpha=\alpha_0+\delta\alpha$, where α_0 is given by Eq. (A3)] leads to a nonvanishing reflection coefficient,

$$|\rho|=\frac{x^2-1}{2}|\delta\alpha|.$$

So, the sensitivity of the reflection coefficient that can be determined as $S=|\rho|/|\delta\alpha|$ grows with an increasing refractive index of the ceramic.

For a double-disk configuration, when the thickness of each disk satisfies condition (A3), the sensitivity of the total reflection coefficient becomes

$$S=\frac{|\rho|}{|\delta\alpha|}=(x^2-1)\,|\cos\beta|.$$

It follows that by choosing the distance between disks, satisfying the condition $k_z L=(l+\frac{1}{2})\pi$ with l=integer, one can have a very insensitive low-reflective output window.

In the case when the window is matched due to the choice of this distance according to condition (A4), the reflection coefficient caused by perturbation in α and β is equal to

$$|\rho|=\left(\frac{8(x^2-1)}{|[(1+x)^2-(1-x)^2\exp(i2\alpha_0)]^2-\{(1-x^2)[1-\exp(i2\alpha_0)]\}^2\exp(i2\beta_0)|}\right)$$
$$\cdot\{[2x\sin\alpha_0\cos\beta_0+(1+x^2)\cos\alpha_0\sin\beta_0]\delta\alpha+[2x\cos\alpha_0\sin\beta_0+(1+x^2)\sin\alpha_0\cos\beta_0]\delta\beta\}. \quad \text{(A5)}$$

Since the value of β_0, as it follows from the condition (A4), may be expressed as the function of α_0 and x (or vice versa, α_0 as a function of β_0 and x), one can find from Eq. (A5) the partial sensitivities of the reflection coefficient ($|\rho|/\delta\alpha$ and $|\rho|/\delta\beta$) as functions of only two parameters: α_0 and x (or β_0 and x).

When the output window is well matched for the operating mode, we can apply the results obtained to determine the reflection coefficients for parasitic modes. For modes generated due to conversion of the operating mode in the irregular waveguide $\delta\alpha=\Delta k_z\, d/x$ and $\delta\beta=\Delta k_z L$, where

$$\Delta k_z=\frac{k_{10}^2-k_{11}^2}{2k_{z0}}=\frac{\nu_0^2-\nu_1^2}{2k_{z0}r_w^2}. \quad \text{(A6)}$$

Here $k_{\perp 0,1}$ are the transverse wave numbers of the operating and parasitic modes, respectively; $\nu_{0,1}=k_{\perp 0,1}r_w$ are the eigenvalues of these modes, i.e., $p_{0,1}$'th roots of the $J'_m(\nu_{0,1})=0$ that is the boundary condition for the $TE_{m,p_{0,1}}$ mode in the waveguide with radius r_w. Note that these modes have the same frequency.

When we consider the parasitic mode that can be excited in the cavity, we must take into account that such a mode has not only a different $k_\perp$ but also a different frequency. Inasmuch as the frequency of this parasitic mode must be close to the frequency of the operating mode because the cyclotron resonance band of the electron beam in gyrotrons is rather narrow, we can assume that both differences between parasitic and operating modes in $k_\perp$ and ω are small enough. Correspondingly, assuming that in the cold-cavity approximation these modes have identical axial structures of the rf field in the resonator (and, hence, the equal axial wave numbers there), we can easily obtain the following expression for the difference between their axial wave numbers in the output waveguide,

$$\Delta k_z=\left(\frac{1}{r_c^2}-\frac{1}{r_w^2}\right)\frac{\nu_0\,\Delta\nu}{k_{z0}}, \quad \text{(A7)}$$

where $\Delta\nu=\nu_1-\nu_0$, r_c is the cavity radius. Since $r_w \gg r_c$, we can neglect the last term in Eq. (A7) and conclude that in such a case the main effect is caused by the difference in mode frequencies.

[1] P. Muggli, M. Q. Tran, T. M. Tran, H.-G. Mathews, G. Agosti, S. Alberti, and A. Perrenoud, IEEE Trans. Microwave Theory Technol. **MTT-38**, 1345 (1990).
[2] K. Felch, R. Bier, L. J. Craig, H. Huey, L. Ives, H. Jory, N. Lopez, and S. Spang, Int. J. Electron. **61**, 701 (1986).
[3] B. Jödicke, Ph.D. thesis, University of Karlsruhe, KfK 4603, 1987.
[4] V. A. Flyagin, V. V. Alikaev, K. M. Likin, G. S. Nusinovich, V. G. Usov, and S. N. Vlasov, *Proceedings of the 3rd Joint Varenna–Grenoble International Symposium, 1982* (Commission of the European Communities, CEN, Grenoble, France, 1982), p. 1059.
[5] M. Thumm, Int. J. Electron. **61**, 1135 (1986).
[6] V. A. Flyagin and G. S. Nusinovich, Proc. IEEE **76**, 644 (1988).
[7] P. B. Sushilin, A. Sh. Fix, and V. V. Parshin, in *Gyrotrons*, Book of Collected Papers (IAP, Gorky, USSR, 1989), p. 181 (in Russian).
[8] L. Rebuffi, *16th International Conference on Infrared and MM Waves, Conference Digest,* Lausanne, Switzerland, edited by M. R. Siegrist, M. Q. Tran, and T. M. Tran (CRPP Ecole Polytechnique Federale de Lausanne, Lausanne, 1991), p. 441.
[9] M. K. Ferber, H. D. Kimrey, and P. F. Becher, J. Mat. Sci. **19**, 3767 (1984).
[10] H.-U. Nickel and M. Thumm, in Ref. 8, p. 444.
[11] G. S. Nusinovich, Int. J. Electron. **51**, 457 (1981).
[12] G. Saraph, T. M. Antonsen, Jr., B. Levush, and G. I. Lin, IEEE Trans. Plasma Sci. **PS-20**, 115 (1992).
[13] Sh. E. Tsimring, in Ref. 7, p. 113, *Gyrotrons.*
[14] K. E. Kreischer, B. G. Danly, P. Woskoboinikow, W. J. Mulligan, and R. J. Temkin, Int. J. Electron. **57**, 851 (1984).
[15] K. Felch, C. Hess, H. Huey, E. Jongwaard, H. Jory, J. Neilson, R. Pendletron, and M. Tsiruluikov, *15th International Conference on Infrared and Millimeter Waves, Conference Digest,* edited by Richard J. Temkin, Proceedings of the SPIE (SPIE, Bellingham, WA, 1990), Vol. 1514, p. 315.
[16] J. D. Jackson, *Classical Electrodynamics* (Wiley, New York, 1975), Chap. 7.